Performance Comparison of PI and PI-Fuzzy Controller for Grid-Connected Fuel Cell Inverter System

N. A. Zambri, M. N. Ismail
Faculty of Electrical and Electronic Engineering
Universiti Tun Hussein Onn Malaysia.
aira@uthm.edu.my, nafis@uthm.edu.my

Azah Mohamed
Department of Electrical, Electronic and Systems Engineering,
Universiti Kebangsaan Malaysia.
azah@eng.ukm.my

***Abstract*- This paper presents the modeling, simulation, and performance evaluation of a hybrid proton exchange membrane fuel cell (PEMFC) with an energy storage system utilized in a grid-connected distributed generation (DG) system. To control the fuel cell/battery grid-side voltage source inverter (VSI), the conventional voltage-mode and current-mode control schemes with improved proportional-integral (PI)-fuzzy controller for both inner current and outer voltage control loops have been developed. The proposed PI-fuzzy controller has the advantage of fuzzy control while maintaining the simplicity and robustness of the PI controller. The space-vector pulse width modulation technique has been applied to the VSI control to generate a sinusoidal waveform. A comparison has been made between the PI-fuzzy controller and the PI controller in the VSI in terms of the generated total harmonic distortion (THD). The results showed that by applying PI-Fuzzy controller, the voltage and current THD are reduced to 0.40 % and 3.77 %, respectively compared to 0.43 % voltage THD and 14.08 % current THD using the conventional PI controller.**

***Index Terms*- DG, PI-Fuzzy, SVPWM, VSI**

I. INTRODUCTION

In recent years, pollution due to fossil fuel use as well as growing concern about global warming have fast become the primary problems in electricity generation around the world. Integration of renewable energy technology into the utility grid through distributed generation (DG) is widely promoted to meet the increasing electric power demand. Renewable energy or micro sources are clean and abundantly available in nature through sources such as solar, wind, gas micro-turbine, and fuel cell (FC) [1]–[2]. Among the many types of renewable energy, fuel cell is a popular candidate for DG applications because of its advantages, which include high efficiency, high power density, silent technology, clean operation, and immunity to weather conditions. To achieve a good performance when increasing the electrical load, the ESS needs to be combined with the FC system as a hybrid configuration [3]. The hybrid FC and energy storage system (ESS), as a DG system, maximizes the benefits of each device in extending battery life and decreasing stress on the FC unit, which improves the system's reliability, integrity, and efficiency, as well as reduces the cost of the system [4]. Once a hybrid DG is connected to the utility grid, operation and performance requirements are imposed on the DG system [5], a crucial part of which is the inverter of the grid interfacing system and the control of power electronics equipment.

In a DG system, the PI controller is widely used to control the firing angle (δ) and the modulation index (m) of the inverter [6]-[7]. Nehrir et al. presented the modeling and the control of the PEMFC-based DG system on the AC grid with real and reactive power control capabilities through a conventional PI controller for DC/DC converters, as well as a direct quadrature transformed two-loop current control scheme for the inverter [6]. PI controllers are also used in [7] to control the real and reactive power in DC/DC boost converters and sinusoidal pulse width modulation two-level inverters in PEMFC-based DG models. However, the tuning process for the PI controller is crucial in obtaining a decreased total harmonic distortion (THD), and this controller type is limited by efficiency loss in non-linear system management.

Intelligent controllers based on fuzzy logic improved the performance of the hybrid FC battery system in [8], in which the fuzzy logic algorithm determined the FC output power relative to the battery state of charge and the external power requirement for improved system efficiency. In [9], fuzzy controller was also employed to handle power flow between the FC and super capacitor (SC) in the DC bus. However, the fuzzy controller fails to respond to a system with rapid dynamic response in the DG application. In addition, an intelligent controller normally requires a complex control algorithm and many parameters require tuning. Such requirements present major difficulties in designing the entire system.

This paper presents modeling and simulation of a FC hybrid DG system with a lead-acid battery for grid-connected operation. The VSI employed a PI-Fuzzy controller in the outer and inner loop controls, and the control gains of the proposed PI-Fuzzy are self-tuned based on the PI controller guideline, which combines the advantages of the fuzzy and PI controllers. These controllers are used with the application of a space vector pulse width modulation (SVPWM) to generate the sinusoidal output waveform. Comparisons are made between the PI-Fuzzy and PI controllers, and between the use of sinusoidal pulse width modulation (SPWM) and SVPWM in the VSI system in terms of the system THD values.

.

II. SYSTEM CONFIGURATION AND MODELING

A. Overview

The configuration of the grid-connected hybrid FC with battery energy storage is shown in Figure 1. The configuration consists of an FC dynamic model, a DC/DC boost converter with a MPPT controller; a VSI which interfaces the FC to the utility grid; and a lead-acid battery with a bidirectional buck/boost converter for DC bus interfacing. With this configuration, the battery functions as backup power to stabilize the system's power flow for load voltage regulation. An ideal three-phase voltage source is applied to the system that represents the external utility grid, which is assumed as an infinitely stiff AC system. In this paper, focused will be the VSI controller design and the model of a hybrid FC/battery system can be seen in [3].

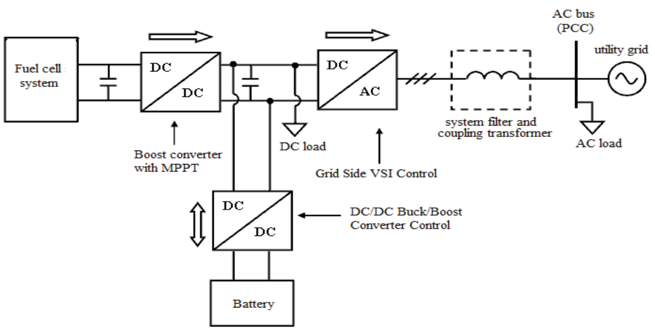

Figure 1. System configuration of a grid-connected FC with battery energy storage

B. Grid-Side Inverter Model

For grid-connected operation, the VSI and its controller are the main important features in designing a power electronic component for DG and grid coupling. The controller is normally realized in the *dq* platform. Considering the simplicity in designing the controller and VSI modeling in [10], a new PI-Fuzzy controller is adopted in this study. The active (P) and reactive (Q) power flow is controlled with the principle of transferring all available power at the constant DC bus to the grid. The control system ensures that a smooth power flow is injected into the utility grid and maintains it at unity power factor. An important aspect that should be considered in grid connection is synchronization of the DG and the utility grid. To achieve an operation with unity power factor, the grid current reference signal must be in phase with the grid voltage, and the synchronization can be conducted by using a phase-locked loop (PLL) topology.

The control method employs the PLL at the point of common coupling to extract the voltage, $vg\_d=|vg\_d|$ and $vg\_q=0$. When any large transient current during faults and sudden load changes occur, applying this technique ensures that the controller will force a direct regulation on the VSI current that will directly avoid the vulnerability of VSI valves. When the system is operating in grid-connected mode, the PLL tracks the grid voltage to ensure synchronization. However, when the hybrid system enters the islanding condition, the PLL for the VSI will change the frequency that is sent to the integrator for angle calculation by another fixed external reference, (ω_{set}), as shown in Figure 2. The proposed VSI with its controller configuration is shown in Figure 3.

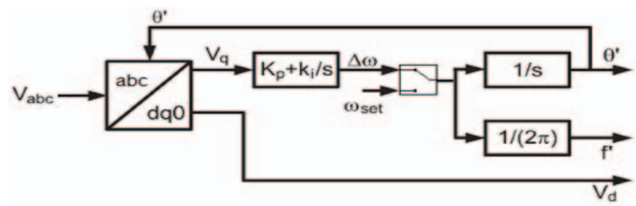

Figure 2. VSI dq-PLL configuration

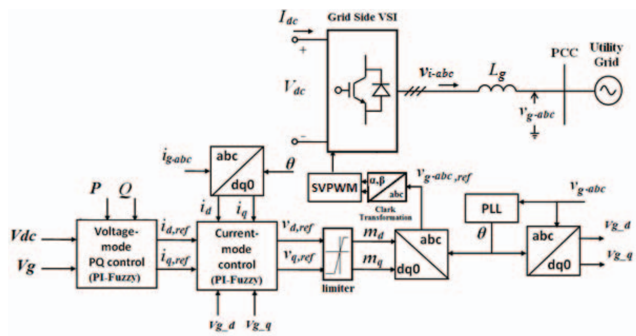

Figure 3. Grid-side VSI control scheme

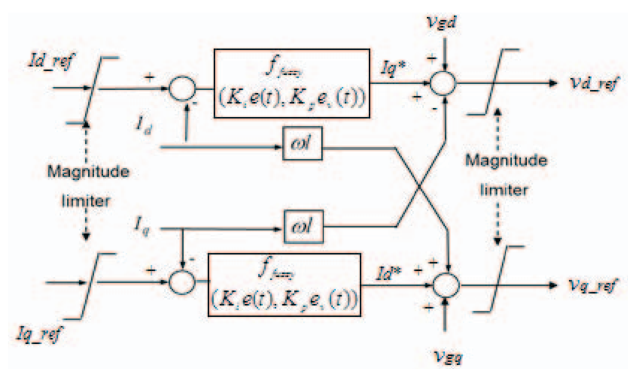

Figure 4. Grid-side VSI control scheme

A. PI-Fuzzy Controller

Three PI-Fuzzy controllers are utilized for the VSI control strategy. Two of the PI-Fuzzy controllers are employed for the inner current control loop to compensate for the error signal of $e_d= I_{d\_ref}-I_d$ and the *q*-reference frame of $e_q= I_{q\_ref}- I_q$, shown in Figure 4, and the configuration of the PI-Fuzzy control for the inner current controller is illustrated in Figure 5. In the outer voltage control loop shown in Figure 6, one PI-Fuzzy controller is utilized to compensate for the voltage error in generating the reference current in the *d*-coordinate, as shown in Figure 7.

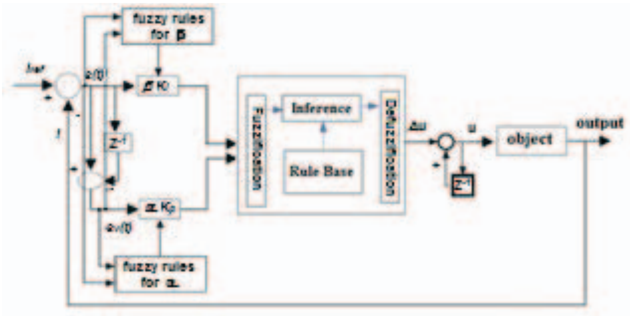

Figure 5. Structure of PI-Fuzzy controller for inner current control

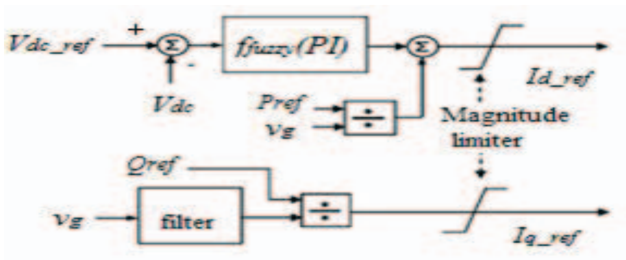

Figure 6. Inverter outer voltage control loop

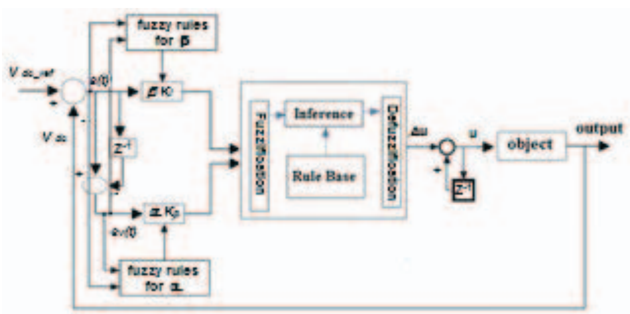

Figure 7. Structure of PI-Fuzzy controller for outer voltage control

The proposed PI-Fuzzy controller for the inner and outer loop controls in the VSI employed the same configuration. The operation of the proposed PI-Fuzzy controller can be written as:

$$u(t) = u(t-1) + \Delta u(t) \quad (1)$$

where t is the sampling instance and Δu is the additional changes in the controller output. From Figure 5 and Figure 7, the delay ratio error [$e(t)$] is multiplied by βK_i and the error rate inputs [$e_v(t)$] by αK_p, where K_p and K_i refer to the proportional and integral gains, respectively while α and β are the gain updating factor for any changes of $e(t)$ dan $e_v(t)$which will be directly calculated using fuzzy logic rules at every sampling times. With the existence of α and β, the value of αK_p and βK_i will be directly self-tuned depends on the changes of the desired input and output. The proposed controller consists of three main design steps, namely, fuzzification, inference, and defuzzification.

a) Outer Voltage Control

The first step is the fuzzification process in which the membership functions for the input and output variables are designed. For the outer voltage control membership functions, the linguistic variables for two fuzzy inputs and one output are indicated by E, EC, and U, which refer to $e(t)$, $e_v(t)$, and output, respectively. The membership functions for two inputs and one output for the outer voltage control loop for the VSI are shown in Figures 8 and 9. The controller output equation is stated as follows:

$$\Delta u(t) = K_p(e(t) - e(t-1)) + K_i e(t) \quad (2)$$

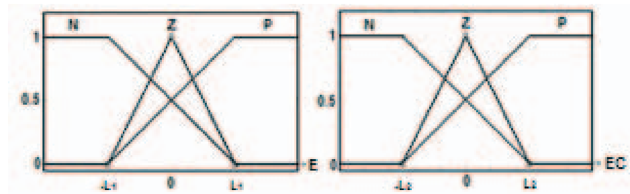

Figure 8 Membership functions for E and EC

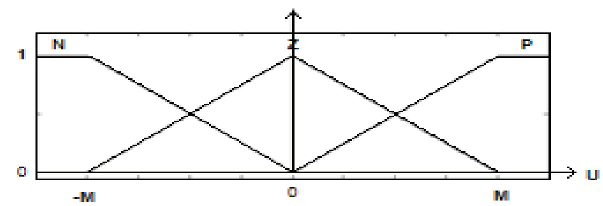

Figure 9 Membership functions for U

From Figure 8, given that *E* is the delay ratio error and *EC* is the error rate input, L_1 and L_2 are both interpreted as the maximum value of $K_i e(t)$ and $K_p e_v(t)$, respectively. In the proposed control, the range of [−10, 10] is utilized in the controller, where the value is selected through experimentation to find the optimum output of the controller. Therefore, L_1 and L_2 are expressed as L_1=10K_i and L_2=10K_p, and the value of M in the membership output function is set as 7.5 and this value is determined from simulation which only utilize PI controller. The result verifies that the selected values are acceptable referred to the lower harmonic component.

For updating α and β values, the similar membership function of *E* and *EC* are used with the value of L_1 and L_2 are set to 5. However, membership function for the output, *U* is shown in Figure 10 in which the range of [-0.5, 1.5] is applied using two fuzzy logic sets which are big (B) and small (S) for α. To determine updating factor of β, range between [0.5, 2.5] is used with three fuzzy logic sets which are big (B), medium (M) and small (S).

The second step is choosing the inference of the controller, and the action of the fuzzy controller is set by employing if–then rules. The rules developed for the outer voltage control are illustrated in Table 1. Rules for α and β are determined using step response effect from the initial simulation. If the system response is slow, the value of *e(t)* need to be increased and $e_v(t)$decreased. Therefore, when E positive (P) and EC negative (N, Z), α will be S and β is B. So, αK_p will decrease to reduce $e_v(t)$ and βKi will rise to increase $e(t)$and vice versa. The last step is the defuzzification process, which involves converting the fuzzy output. The following formula is employed to defuzzify the incremental control of fuzzy control law:

$$U = \frac{\sum b_i.\mu_i}{\sum \mu_i} \quad (3)$$

where b_i is the output for Rule i and μ_i refers to the corresponding membership value for Rule i. μ_i is computed by employing the intersection of the fuzzy sets E and EC denoted by $E \wedge EC$ and can be defined by the following:

$$\mu_i(E) \wedge \mu_i(EC) = \min(\mu_i(E) \wedge \mu_i(EC)) \quad (4)$$

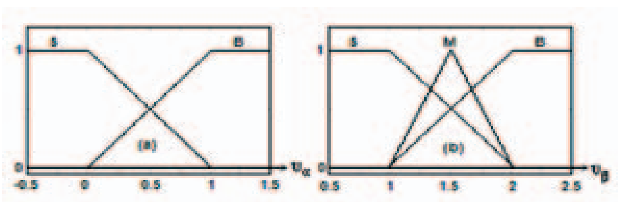

Figure 10. Membership function for U (a) to determine α (b) to determine β

TABLE I. FUZZY RULES FOR OUTER VOLTAGE CONTROL

		EC		
	Rules for I_{d_ref}	N	Z	P
E	N	N	N	Z
	Z	N	Z	P
	P	N	P	P

b) *Inner Current Control*

The similar step applied for the outer voltage control is used for the inner current control in constructing PI-fuzzy controller. Membership function for two inputs are similar to the outer voltage control and one output for inner current control are shown in Figure 11.

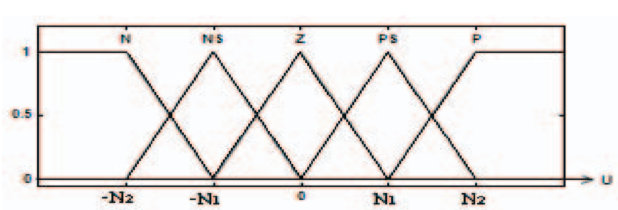

Figure 11. Membership functions for U in inner current control

There are two coordinates that need to be controlled which are d and q. Range of [-10, 10] is used for both coordinates and the value of N_2 and N_1 in Figure 11 are set as N_2=10 and N_1=5, respectively for dq-coordinates. Fuzzy logic rules for both coordinates are shown in Table 2 in which N, Z, P, NS and PS are negative, zero, positive, negative small and positive small, respectively. For updating α and β values, membership functions used are similar to the outer voltage control. However, different fuzzy rules are used in determining α and β for dq-coordinates and shown in tables 3 and 4.

TABLE II. FUZZY RULES FOR INNER CURRENT CONTROL IN *dq*-COORDINATE

		EC					*EC*		
	Rules for I_d*	N	Z	P		Rules for I_q*	N	Z	P
E	N	N	NS	NS	E	N	N	Z	NS
	Z	NS	Z	PS		Z	NS	Z	PS
	P	Z	PS	P		P	PS	PS	P

TABLE III. FUZZY RULES FOR DETERMINING α and β FOR INNER CURRENT CONTROL IN *d*-COORDINATE

		EC					*EC*		
	Rules for α	N	Z	P		Rules for β	N	Z	P
E	N	S	S	S	E	N	B	B	M
	Z	S	S	B		Z	B	B	S
	P	S	B	B		P	M	S	S

TABLE IV. FUZZY RULES FOR DETERMINING α and β FOR INNER CURRENT CONTROL IN *q*-COORDINATE

		EC					*EC*		
	Rules for α	N	Z	P		Rules for β	N	Z	P
E	N	B	B	B	E	N	S	S	M
	Z	B	B	S		Z	S	B	B
	P	B	S	S		P	M	B	B

B. *SVPWM*

The SVPWM is the best method among all the PWM techniques for generating the sinusoidal wave for power electronic converter. The SVPWM has been proven to decrease harmonic content, minimize bus utilization, achieve precise control, and lower switching losses [11]–[13]. The SVPWM model is based on the instantaneous values of the reference voltages of a, b, and c only, and the orthogonal coordinates are utilized to represent the three-phase voltage vector in the phasor diagram, as illustrated in the following equations:

$$U_\alpha = \frac{2}{3}(v_{ao} - 0.5v_{bo} - 0.5v_{co}) \quad (5)$$

$$U_\beta = \frac{2}{3}(\frac{\sqrt{3}}{2}v_{bo} - \frac{\sqrt{3}}{2}v_{co}) \quad (6)$$

In the SVPWM configuration, the reference vector (U_{ref}), which rotates at an angular speed of $2\pi f$, represents the three-phase output voltage. The rotating reference vector will be switching between the adjacent six active vectors and two zero vectors, and the equations below will determine the sector (N) in which the reference voltage vector is in.

$$U_{ref1} = U_{\beta} \tag{7}$$

$$U_{ref2} = \frac{\sqrt{3}}{2}U_{\alpha} - 0.5U_{\beta} \tag{8}$$

$$U_{ref3} = -\frac{\sqrt{3}}{2}U_{\alpha} - 0.5U_{\beta} \tag{9}$$

Redefining,

If $U_{ref1} > 0$, A=1, or else A=0 (10)

If $U_{ref2} > 0$, B=1, or else B=0 (11)

If $U_{ref3} > 0$, C=1, or else C=0 (12)

The sector mapping (S) for the neutral voltage of phases A, B, and C is described as follows:

$$S = A + 2B + 4C \tag{13}$$

S can be the six-integer value from sectors 1 to 6. Figure 12 shows the sector correspondence diagram with the six non-zero vectors (V_1–V_6) and two-zero vectors (V_0 and V_7). The figure shows that the angle between two active vectors or non-zero vectors is 60 degrees and will feed electrical power to the load. Meanwhile, the two zero vectors are at the origin and will feed zero voltage to the electrical load. Normally, the main objective in SVPWM is to approximate the reference voltage vector that employs the eight switching patterns. The next step in developing SVPWM is to determine the three time durations (T_1, T_2, and T_0). The switching time duration at any sector in the diagram is shown in the following equations:

$$T_1 = \frac{\sqrt{3}T\left|\overline{U}_{ref}\right|}{V_{dc}}\left(\sin\frac{n}{3}\pi kos\alpha - kos\frac{n}{3}\pi\sin\alpha\right) \tag{14}$$

$$T_2 = \frac{\sqrt{3}T\left|\overline{U}_{ref}\right|}{V_{dc}}\left(kos\alpha.\sin\frac{n-1}{3}\pi + \sin\alpha.kos\frac{n-1}{3}\pi\right) \tag{15}$$

$$T_0 = T_Z - T_1 - T_2 \tag{16}$$

The last step is to determine the three-phase correspondence switching times (T_{cm1}, T_{cm2}, and T_{cm3}) by employing the asymmetric SVPWM switching pattern, for the six transistors in the three-phase inverter. From the asymmetric SVPWM switching pattern [12], the following equations are obtained:

$$T_a = (T_o - T_1 - T_2)/2 \tag{17}$$

$$T_b = T_a + T_1 \tag{18}$$

$$T_c = T_b + T_2 \tag{19}$$

Referring to the switching pattern at each sector can derive the three-phase switching time for phases A, B, and C, which are defined as T_{cm1}, T_{cm2}, and T_{cm3}, respectively, according to Table 4.With the application of a step-by-step technique and the use of Equations (5) to (19), the SVPWM for generating the sinusoidal wave for the three-phase inverter is simulated by using the MATLAB/Simulink software to minimize the harmonic component in the grid voltage and current.

III. SIMULATION MODEL

A complete system model composed of a grid-connected hybrid PEMFC model coupled with a lead-acid battery model for DG applications was developed, and the overall performance of the developed system is simulated by using MATLAB/Simulink, which offers a graphical interface as block diagrams. This software allows the user to view the system at different levels, such that the models are easily joined together. During simulation, the parameters can be changed, and the results generated from different simulations are eventually analyzed. With the application of the PEMFC, lead-acid battery, battery converter models, grid inverter, and entire power electronic controller described earlier, the complete hybrid system is implemented in the MATLAB/Simulink environment.

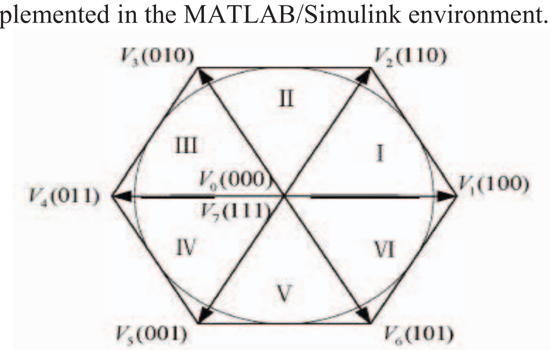

Figure 12. Basic switching vector and sector diagram

TABLE V. THREE-PHASE SWITCHING TIME OF THE SVPWM

Time	Sector					
	I	II	III	IV	V	VI
T_{cm1}	T_a	T_b	T_c	T_c	T_b	T_a
T_{cm2}	T_b	T_a	T_a	T_b	T_c	T_c
T_{cm3}	T_c	T_c	T_b	T_a	T_a	T_b

IV. SIMULATION RESULTS

This section provides a simulation results on the overall performance of the studied system with the proposed control strategy occurred on a complete hybrid PEMFC and a lead-acid battery system for a grid-connected analysis of a DG system. In this simulation, the comparison of the overall system using conventional PI controller and proposed PI-fuzzy controller has been made and two main conditions are considered. The first result is the THD comparison of the complete system using conventional PWM system and the second result is the THD comparison using SVPWM.

A comparison is conducted for THD value on the hybrid system between the PI-Fuzzy controller and the PI controller and between the sinusoidal PWM and the SVPWM in the VSI system. The results of the harmonic components using sinusoidal PWM and SVPWM are tabulated in Table 6. The worst THD value for current (THDi) occurs by applying the classical PI controller with sinusoidal PWM of 14.08%, whereas the THD value for voltage (THDv) is quite satisfactory at 0.43%.

TABLE VI. PERFORMANCE COMPARISON OF THD FOR PI AND PI-FUZZY CONTROLLER

Controller	PI			PI-Fuzzy		
THD	V (%)	I (%)	Fund. For I (p.u)	V (%)	I (%)	Fund. For I (p.u)
SPWM	0.43	14.08	0.7622	0.42	6.14	0.8724
SVPWM	0.42	8.36	0.7932	0.40	3.77	0.9423

When the sinusoidal PWM is substituted with the SVPWM, the current THD decreases to 8.36% and the THD for voltage decreases to 0.42%. Subsequently as PI-Fuzzy replaces the conventional PI controller, the parameters are improved with reduction of THDi at 6.14% while the SPWM technique is applied to generate the sinusoidal waveform. It shows here that by applying PI-Fuzzy approach, the harmonic component is reduced and this controller is suitable for the VSI application. When the PI-Fuzzy controller is used with SVPWM, the value further decreased to 3.77% for current and 0.40% for voltage. The fundamental value for current increase from 0.7622 p.u by applying PI controller with SPWM to 0.9423 p.u by applying PI-Fuzzy controller with SVPWM and consequently higher output current can be achieved by applying SVPWM compared to SPWM. According to IEEE Standard 519-1992, the limits for THDv and THDi are both set at 5% and 20%, respectively and from the results obtained all are acceptable and satisfactory. In addition, the harmonics component have to be lower enough because higher harmonics value will perform malfunction to other equipment and also increase heat losses in transformers and wires. The control technique for VSI application plays an important role in minimizing the harmonic component being injected to the utility grid. The proposed PI-Fuzzy control technique was successful with fewer harmonics current being injected into the grid.

CONCLUSION

The challenge for renewable energy technology integration relies on the manner of managing and developing the control strategy for the whole system and power electronic equipment. For a grid connected hybrid FC and battery system, the control goals are regulation of the DC bus and lowering the harmonic component injected to the utility grid. In this paper, a hybrid PEMFC and battery energy storage system for a grid-connected DG configuration are developed and simulated by employing the MATLAB/Simulink software. An improved PI-Fuzzy controller has been proposed with the existence of SVPWM for generating the sinusoidal form to reduce total harmonic distortion of the system. The proposed PI-Fuzzy control is simpler and can be easily tuned during any uncertainties. The harmonic study on the hybrid system shows that using the proposed control results in lower harmonic current and voltage injected to the grid compared with those of the conventional control.

ACKNOWLEDGEMENTS

The authors would like to thank the Universiti Tun Hussein Onn Malaysia (UTHM) for their support for this work.

REFERENCES

[1] G. Joos, B. T. Ooi, D. Mcgillis, F. D. Galiana, R. Marceau, "The potential of distributed generation to provide ancillary services," in *2000 IEEE Power Engineering Society Summer Meeting*, pp. 1762-1767.

[2] J. J. Brey, A. Castro, E. Moreno, C. Garcia, "Integration of renewable energy sources as an optimised solution for distributed generation", in *2002 28th IEEE Annual Conference of the Industrial Electronics Society*, pp. 3355-3359.

[3] N. A. Zambri, A. Mohamed, H. Shareef, M. Z. C. Wanik, "Design of a Hybrid Fuel Cell with Battery Energy Storage for Stand-Alone Distributed Generation Applications", World Academy of Science, Engineering and Technology, vol. 1, pp. 1588 – 1594, 2013.

[4] T. Yalcinoz, M. S. Alam, Improved dynamic performance of hybrid PEM fuel cells and ultracapacitors for portable applications, International Journal of Hydrogen Energy (2008) 1932-1940.

[5] A. Hajizadeh, M. A. Golkar, "Intelligent Power Management Strategy of hybrid Distributed Generation System", International Journal of Electrical Power and Energy Systems, vol. 29, pp. 783–795, 2007.

[6] M. H. Nehrir, C. Wang, H. Gao, "Control of PEM fuel cell distributed generation systems", IEEE Transactions on Energy Conversion, vol. 21, pp. 586- 595, 2006.

[7] W. T. Ghareeb, F. M. Bendary, E. M. Saied, Y. G. Hegazy, "Investigating the performance of a fuel cell based distributed generation system",in *2010 Energy Conference and Exhibition*, pp. 462-467.

[8] J. Kwi-Seong, L. Won-Yong, K. Chang-Soo, "Energy management strategies of a fuel cell/battery hybrid system using fuzzy logics", Journal of Power Sources, vol. 145, pp. 319-326, August 2005.

[9] A. Hajizadeh, M. A. Golkar, "Control of hybrid fuel cell/energy storage distributed generation system against voltage sag", International Journal of Electric Power and Energy Systems, vol. 32, pp. 488-497, june 2010.

[10] M. Z. C. Wanik, "Dynamic Simulation and Intelligent management of Distributed Generation", Ph.D thesis, Duisburg-Essen University, Germany, 2011.

[11] X. Shaobang, H. Ke-You, "Research on a Novel SVPWM Algorithm", in *Proc. of 2007 Second IEEE Conference on Industrial Electronics and Applications*, pp. 1869-1887.

[12] A. Iqbal, A. Lamine, I. Asharf , Mohibullah, "MATLAB/SIMULINK model of space vector pwm for three phase voltage source inverter", in *Proc 2006 UPEC*, pp. 1096-1100.

[13] Z. Wei-Feng, Y. Yue-Hui, "Comparison of Three SVPWM Schemes", in *2007 Proc of Journal of Electronic Science and Technology fo China*, pp. 283-287.